proceedings

MDPI

Proceedings

Controlled Release of Cinnamon Leaf Oil from Chitosan Microcapsules Embedded within a Sodium Alginate/Gelatin Hydrogel-Like Film for *Pseudomonas aeruginosa* Elimination †

Catarina S. Miranda, Joana C. Antunes, Natália C. Homem and Helena P. Felgueiras *

Department of Textile Engineering, Centre for Textile Science and Technology (2C2T), University of Minho, Campus of Azurém, 4800-058 Guimarães, Portugal; catarinanda@gmail.com (C.S.M.); joana.antunes@2c2t.uminho.pt (J.C.A.); natalia.homem@2c2t.uminho.pt (N.C.H.)

* Correspondence: helena.felgueiras@2c2t.uminho.pt; Tel.: +351-253-510-283; Fax: +351-253-510-293

† Presented at the First International Conference on "Green" Polymer Materials 2020, 5–25 November 2020; Available online: https://cgpm2020.sciforum.net/.

Published: 3 November 2020

Abstract: *Pseudomonas aeruginosa* is considered a public threat, with antibiotics increasing its resistance. Essential oils (EOs) have demonstrated significant effects against microorganisms. However, due to their volatile nature, they cannot be used in their free-state. Here, hydrogel-like films were produced from a combination of sodium alginate (SA) and gelatin (GN) to serve as delivery platforms for the controlled release of cinnamon leaf oil (CLO) entrapped within chitosan (CS) microcapsules. The minimum inhibitory concentration (MIC) of CLO was established at 39.3 mg/mL against *P. aeruginosa*. CS microcapsules were prepared via ionotropic gelation with tripolyphosphate (TPP), encapsulating CLO at MIC. Successful production was confirmed by fluorescent microscopy using Nile red as detection agent. Microcapsules were embedded within a biodegradable SA/GN polymeric matrix processed by solvent casting/phase inversion with SA/GN used at 70/30 polymer ratio at 2 wt% SA concentration. 2 wt% $CaCl_2$ was used as coagulation bath. The CLO-containing CS microcapsules homogeneous distribution was guaranteed by successive vortex and blending processes applied prior to casting. CLO controlled release from the films was monitored in physiological pH for 24 h. Hydrated films were obtained, with the presence of loaded CS capsules being confirmed by FTIR. Qualitative/quantitative antimicrobial examinations validated the loaded film potential to fight *P. aeruginosa*.

Keywords: bio-based polymers; drug delivery platform; natural extracts; trigger-based release; bactericidal effects.

1. Introduction

Pseudomonas aeruginosa is a Gram-negative, rod-shaped, asporogenous and monoflagellated bacteria of major clinical importance. It is a very powerful opportunistic human pathogen that survives under a great variety of conditions, causing infections, not only in immunocompromised cancer patients but also in patients suffering from burns and cystic fibrosis [1]. *P. aeruginosa*-derived infections are difficult to eradicate due to this bacterium elevated intrinsic antibiotic resistance. As a result, this microorganism is categorized by the Infectious Diseases Society of America as a human pathogen with clinically relevant antibiotic resistance [2,3].

Several antimicrobial agents, including antibiotics, have been used to fight *P. aeruginosa*-related infections. Yet, their excessive consumption and misuse has led to an increased appearance of antibiotic resistance [4]. Hence, the current urgency in finding alternatives. In recent years, natural

products derived from plants, possessing antimicrobial, anti-inflammatory, antioxidant and chemo-preventive properties, have gained a new importance as antibiotic replacements by effectively treating infections and causing little impact in the human health or the environment [5]. Essential oils (EOs) consist of mixtures of aromatic, volatile, lipophilic biomolecules, extracted from different regions of plants, working as secondary metabolites that defend the host from microbial invasions [6]. Many studies have proven their potential to replace antibiotics due to their inherent strong anti-inflammatory, antiseptic and analgesic properties, for instance [7]. However, the cytotoxicity of the EOs at high concentrations, their low resistance to degradation and their high volatility still constitute challenges to overcome prior to their generalized consumption [8].

Polymeric nanocapsules that contain a liquid core surrounded by a polymeric shell have been highlighted as effective drug carriers [9]. By encapsulating antimicrobial agents at the core, these polymeric systems can increase the drug-loading efficiency, decrease the matrix content of the nanoparticles and isolate the encapsulated payload from the surrounding environment. Moreover, this isolation prevents secondary undesirable effects related with early degradation and burst release, which can be induced by external factors, like alterations in pH and temperature, or presence of enzymes [10,11]. The properties of the shell material strongly influence the stability, encapsulation efficiency and release profile of the nanocapsule. Polysaccharides have been commonly used as drug carriers, due to their biocompatibility, gelation conditions and mucoadhesive properties. Furthermore, they possess deprotonated amino groups or carboxylic acid groups, which will turn the surfaces cationic or anionic, enabling the formation of shells by electrostatic interactions [12]. Chitosan is a natural copolymer of glucosamine and N-acetylglucosamine, obtained by deacetylation of chitin, that have the ability to form nanocapsules with a positive surface charge. The cationic surface is responsible for improving the interactions between the nanoparticles and some gram-negative bacteria, through electrostatic interactions, thus increasing its ability to fight infections [13,14].

In this study, an optimized delivery platform was engineered for a targeted and controlled release of cinnamon leaf oil (CLO), a very powerful antimicrobial EO, entrapped within chitosan microcapsules, using hydrogel-like films produced from a combination of sodium alginate (SA) and gelatin (GN). To the authors knowledge, this is the first report on the controlled release of CLO from chitosan microcapsules embedded within a SA/GN matrix for the eradication of *P. aeruginosa* bacteria.

Hydrogel-films are widely used for cell microencapsulation since they present a high porosity that results in a high permeability of oxygen, nutrients and metabolites. SA and GN are commonly used in biomedical applications, due to their biocompatibility and biodegradability [15]. SA is a water-soluble salt and a naturally occurring non-toxic polysaccharide found in brown algae species [1,2], endowed with great biocompatibility, low immunogenicity and minor gelation conditions [14]. SA is frequently used in cell encapsulation since it presents a fast ionic gelation with divalent cations [15]. Nonetheless, alginate alone does not lead to an efficient cell attachment, causing poor cell-material interactions. Furthermore, it presents a slow degradability and uncontrolled degradation kinetics [17]. Therefore, in order to overcome these limitations, GN is frequently applied [18,19]. GN is a biodegradable protein, formed by hydrolysis of collagen, which has been used for controlled drug release due to its biodegradability and biocompatibility [16].

2. Experiments

2.1. Materials

Pure cinnamon leaf oil (CLO, extracted from *Cinnamomum zeylanicum*, $\rho = 1.049$) was purchased from Folha d'Água Company (Portugal). Nutrient broth (NB) and nutrient agar (NA) were acquired from VWR, while Mueller Hinton broth (MHB) was obtained from CondaLab. *P. aeruginosa* bacteria (ATCC 25853) was supplied from American Type Culture Collection (ATCC).

Chitosan (CS, Mw 100–300 kDa, Acros Organics) and sodium tripolyphosphate (TPP, Sigma) were used in the production of the microcapsules. Gelatin (GN, ~300 Bloom, Type A from porcine skin) and sodium alginate (alginic acid sodium salt, SA, from brown algae, ≥ 2,000cP) were purchased

from Sigma and used in the production of the hydrogel-like films. Distilled water (dH_2O) was used as the polymer's solvents, and a 2 wt% solution of calcium chloride ($CaCl_2$ anhydrous, Chem-Lab) was employed as coagulation bath.

2.2. Cell Wall Disruption: Scanning Electron Microscopy (SEM) Observations

To analyze the CLO capacity to interfere with the cell morphology of *P. aeruginosa*, visual studies resorting to SEM were conducted. Bacteria suspensions were prepared at 1×10^7 CFUs/mL in MHB and combined at a 50 % (*v*/*v*) with CLO at the minimum inhibitory concentration (MIC) value, which was previously determined as 39.3 mg/mL [21]. 500 μL of each solution (250 μL CLO + 250 μL bacteria) were left in direct contact with 12-well tissue culture plates (TCPS) and incubated at 37 °C for 24 h at 120 rpm. CLO-free bacteria were used as control. Afterwards, culture media was removed and 500 μL of 2.5 % (*v*/*v*) glutaraldehyde in PBS were added to each sample for 1 h at room temperature (RT), to promote cell fixation to the TCPS wells. Plates were gently rinsed with dH_2O and submitted to a dehydration process using serial ethanol dilutions, 55, 70, 80, 90, 95, 100 % (*v*/*v*), each solution was left in the TCPS for 30 min at RT, and then carefully discarded. After the last solution, the remaining ethanol was evaporated at RT. Discs were cut from the TCPS wells, containing the fixated and dehydrated bacteria, using a hot press-on apparatus and covered with a thin film (10 nm) of Au-Pd (80–20 wt%) in a 208HR high-resolution sputter coater (Cressington Company, Watford WD19 4BX, United Kingdom) coupled to a MTM-20 Cressington high resolution thickness controller. Cell morphology was observed via FEG-SEM (NOVA 200 Nano SEM, FEI Company), using an electron accelerating voltage of 10 kV.

2.3. CLO Encapsulation: Chitosan Microcapsules Production

Prior to any processing, CS was dried at 50 °C for 24 h to eliminate any water trace. For microcapsules production, four processing conditions were selected (Table 1). In all cases, firstly, CS was hydrated in dH_2O for 30 min, and then acetic acid was added dropwise (under strong stirring), and left blending for 2 h. TPP was prepared in dH_2O under slow stirring for 1 h. In case of the CS4 and CS4N solutions, the pH of both CS and TPP was set to 5.0.

CLO was added dropwise to the CS1 and CS4 and left blending for 10 min. In the CS1N and CS4N (Nile Red containing samples), CLO corresponding volumes were also added, and 2 min after its addition, a solution containing Nile Red was added and left under stirring for 8 min. Then, TPP was combined dropwise with all solutions under strong stirring. The solutions were homogenized in an Ultraturrax (T25 digital, IKA®) on a pulsation mode (10 sec ON, 10 sec OFF) repeated 5 times, and then transferred to dialysis membranes (SnakeSkin 10 kDa cut-off, Thermo Fisher). The dialysis was performed in dH_2O and the water was exchanged 3 times during a period of 24 h.

Table 1. CS microcapsules processing conditions (* after pH adjustment).

Sample	CS (mg)	dH_2O (mL)	Acetic acid (μL)	CLO (μL)	Nile Red (μL)	TPP (mL)	pH adjust	NaOH (mL)	dH_2O * (mL)
CS1	2.5	9.9	100	834	-	9	No	-	-
CS1N	2.5	9.9	100	834	166	9	No	-	-
CS4	2.5	6.9	100	834	-	9	Yes	1.1	1.9
CS4N	2.5	6.9	100	834	166	9	Yes	1.1	1.9

2.4. SA/GN Films Production

SA/GN films were produced by mixing the SA and GN solutions in a ratio of 70:30 *v*/*v*. SA (2% *w*/*v*) and GN (~1% *w*/*v*) were dissolved separately in dH_2O at 50 °C under stirring for 3 h and 1 h, respectively. GN was added to the SA solution and blended under slow stirring until a homogeneous solution was obtained (~1 h). The solutions were then poured into glass petri dishes of 140 mm diameter (40 mL), left at 4 °C overnight to remove air bubbles, and subsequently slowly dried at RT for 6 days. A 2 wt% $CaCl_2$ solution was then added to the petri dishes containing the films for crosslinking. After 1 h of contact, the films were detached from the dishes and washed in 100 mL of

dH_2O at 150 rpm for 5 min, a process that was repeated 3 times. To prepare the SA/GN films containing CLO microcapsules, the solutions CS1 and CS4, after being subjected to dialysis, were added to the SA/GN solutions and kept under low stirring for 30 min; their water content was used as complementing solvent for the polymers. The following steps were kept equal to the unloaded films.

2.5. Chemical Characterization: ATR-FTIR

Attenuated total reflectance-Fourier transform infrared spectroscopy (ATR-FTIR) was applied to study the surface chemistry and chemical composition of the films. The wavenumber ranged between 400 and 4000 cm^{-1} using an IRAffinity-1S (Shimadzu, Japan), coupled with a diamond crystal. 200 scans were performed for each film at a spectral resolution of 2 cm^{-1}.

2.6. CLO Release Profile from the Loaded Films

Unloaded and loaded films were incubated at 37 °C and 120 rpm in simulated body fluid (SBF) prepared at physiological pH (7.4). The release of CLO was monitored after 1, 2, 6 and 24 h of incubation. Spectophotometer UV-VIS (UV-1800, Shimadzu) was used to analyze the CLO presence within the SBF (release) overtime at the wavelength of 280 nm (characteristic of CLO) [25].

2.7. Time-Kill Kinetics

P. aeruginosa suspensions were prepared at 1×10^5 CFUs/mL in NB and combined with the CLO or the CLO-loaded films at MIC. Control groups were prepared without the addition of any agent or by using unmodified SA/GN films. Bacteria-containing solutions were incubated at 37 °C and 120 rpm. After 0 (before action), 1, 2, 6 and 24 h of incubation, bacteria were serially diluted (10^1 to 10^5 in PBS), cultured on NA plates and further incubated for another 24 h at 37 °C. Colonies of surviving bacteria were counted and reported as mean ± standard deviation (S.D.). Log reduction determinations were also conducted between unloaded and loaded films and reported as mean ± S.D. Data was collected in triplicate and processed using the GraphPad Prism 7.0 software.

3. Results and Discussion

3.1. Cell Wall Disruption

The CLO interference with the Gram-negative bacteria cell membrane was examined via SEM after 24 h of contact. Figure 1 shows the resulting morphology after contact with CLO at MIC. Prior to any contact with the antimicrobial agent, *P. aeruginosa* bacteria exhibited a rod-like shape structure, typically of ≈2.0 μm long and 0.25–1.0 μm in diameter, with a very smooth and uninterrupted surface. *P. aeruginosa* cells may also present polar flagella that confer the cells with mobility [21,22]. Here, however, those were not detected. Still, many cells revealed signs of undergoing polar binary fission.

CLO, like most EOs, act primarily against the bacteria cytoplasmic membrane by accumulating at the cell surface and disturbing its structure and functionality, increasing the odds of cell content leakage and ultimately cell death [23]. Here, it was evident that CLO increased the *P. aeruginosa* bacteria permeability, deforming its original morphology with the appearance of holes or wrinkles along the membrane. CLO surrounded the cells, isolating them for an effective permeabilization. Since these bacteria are relatively more resistant to hydrophobic biomolecules than Gram-positive bacteria to overcome their impermeability, CLO relied on the cell isolation to slowly traverse the outer cell wall porins and reach the intracellular space [21,24].

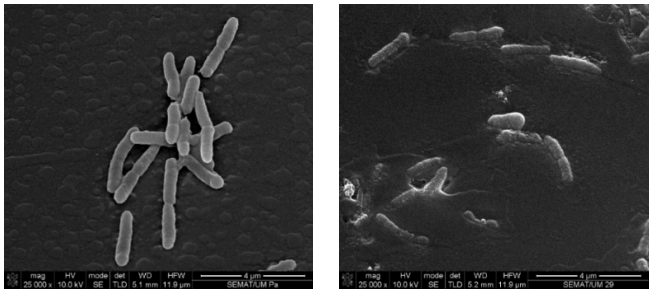

(**a**) (**b**)

Figure 1. Micrographs of the *P. aeruginosa* morphology: (**a**) before and (**b**) after contact with CLO.

3.2. Microcapsules Observation

The microcapsules were observed by Fluorescence Microscopy (DM IL LED, Leica Mycrosystems) with 40 x magnification. Figure 2 represents the morphology of CS1 and CS4 samples before and after dialysis, prior to their incorporation onto films and to any contact with *P. aeruginosa*. For both samples (CS1 and CS4) it was evident that the non-reacted polymer was eradicated after dialysis (Figure 2b,d). Furthermore, it is visible that the sample CS4 contains larger microcapsules and more unloaded chitosan aggregation (Figure 2c,d) than CS1. Therefore, it was concluded that the production of the samples without pH adjustment (CS1) was more effective.

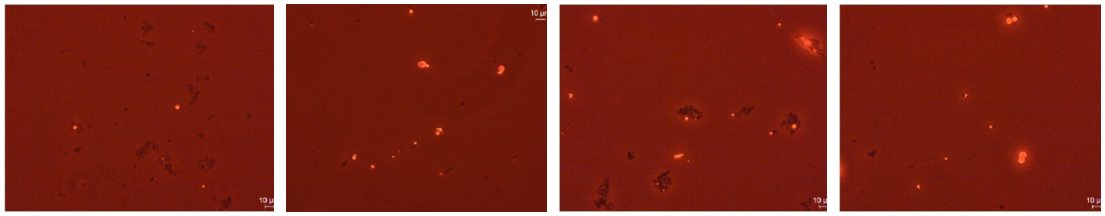

(**a**) (**b**) (**c**) (**d**)

Figure 2. CS1 and CS4 morphology (**a**,**c**) before and (**b**,**d**) after dialysis, respectively.

3.3. Chemical Characterization

ATR-FTIR spectra of the SA/GN films unloaded with loaded with CS1 and CS4 were collected (Figure 3). A slightly broad band centered at ≈3420 cm^{-1} was observed in all spectra and it was attributed to the hydrogen bonded O–H stretching vibrations. It was explained by the polymers' affinity to water molecules. Characteristic peaks of each individual polymer were detected at 1416 and 1036 cm^{-1} for SA, attributed to the symmetric stretching vibration of the carboxylate group and the C-O stretching vibrations [15], respectively, and at 1225 and 1063 cm^{-1} for GN, which revealed the presence of amide III (corresponding to the stretching bonds of C-H and bending bonds of N-H) and C-O stretching vibrations [18,19], respectively. Presence of CLO was detected by the appearance of a peak at 1724 cm^{-1}, which was assigned to the C=O stretching vibrations of the oil components, and the presence of a very smooth peak at 1543 cm^{-1}, which is attributed to the aromatic ring C=C skeleton vibration of an aromatic substance [4]. CLO was more easily noticeable on the CS4-containing films than on the CS1, which may indicate that the EOs molecules were larger.

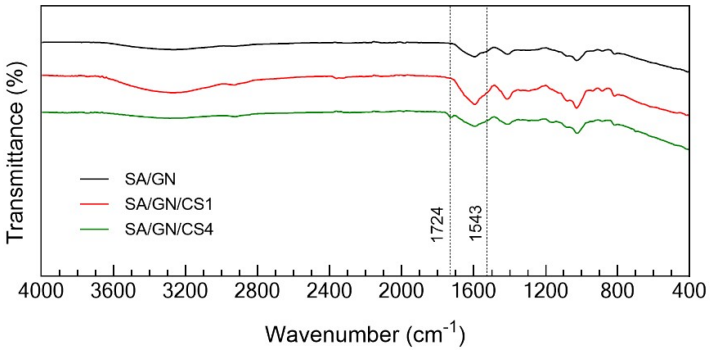

Figure 3. ATR-FTIR spectra of the SA/GN unloaded and loaded with CS1 and CS4.

3.4. CLO Release Profile

The CLO release profile from the CS1 and CS4 loaded films in the presence of SBF was assessed for a period of 24 h (Figure 4). The influence of SA and GN was considered and eliminated from the obtained profile. SA/GN/CS1 released the CLO gradually, in a constant-like manner, with the strongest burst release being detected at the 2 h period and reaching an equilibrium within the 24 h. On the other hand, the SA/GN/CS4 samples, were only able to start releasing the CLO after 2 h. For the entire test, their release profile was always inferior to that of the CS1-containing films. This occurred because when the CS and TPP pH's were adjusted to 5, a stronger interaction between the capsules and the polymeric matrix of the films was achieved, thus narrowing CLO's release. Also, at this pH the higher presence of clusters (as observed in Figure 2) may have reflected in a greater oil retention under the tested conditions.

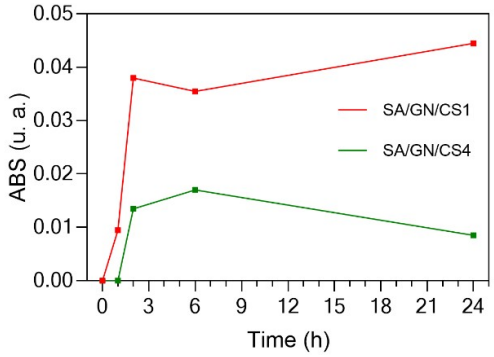

Figure 4. CLO release profile from 1 h to 24 h of incubation in SBF.

3.5. Time-Kill Kinetics

The time-kill kinetics of the loaded films was determined by the number of remaining viable cells at specific incubation periods, 1, 2, 6 and 24 h (Figure 5). The relative log reduction between the unloaded and loaded films was also verified. In the first hour of interaction, all films promoted the bacteria growth. However, as the release of the CLO from the films intensified (Figure 4), so did its action against the bacterium. Indeed, at the 2 h target the SA/GN/CS1 experienced a significant reduction in the number of viable bacteria. Further, its log reduction became significantly enhanced in comparison to the CS4-loaded films. From 6 h to 24 h the reduction of viable cells continued. The main component of CLO, the eugenol is known to interfere with the cells intracellular functions or ions transport, this way preventing important metabolites and connection pathways from taking place and, ultimately, leading to the cell death [4]. Still, due to the reduced release of the CS4 from the films after 6 h, the action against the bacterium became compromised on the CS4-containing films,

allowing viable cells to continue multiplying and increasing their number in the media. Once again, the presence of agglomerates that surrounded the CLO-loaded microcapsules may have prevented their release and consequent effective action.

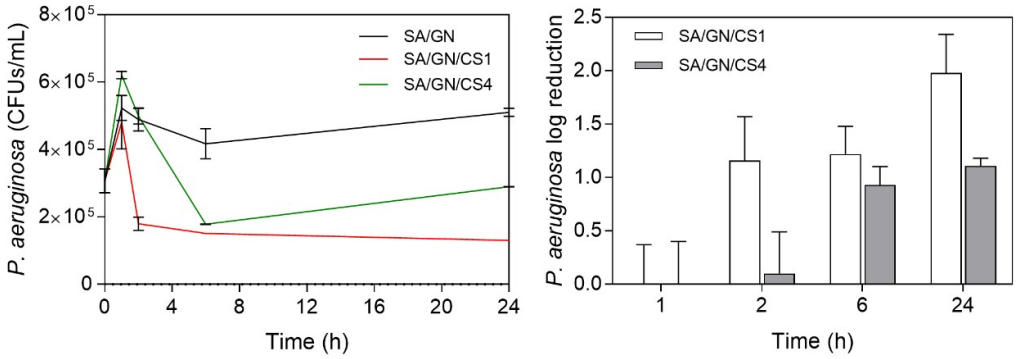

Figure 5. Time-kill kinetics of the *P. aeruginosa* bacteria in contact with the unloaded and loaded films and log reduction of the loaded films in relation to the control (unloaded SA/GN).

4. Conclusions

In the end of this research, it was confirmed the incorporation of the CLO-containing CS microcapsules within the SA/GN fibers. The continuous release of the entrapped oil over a period of 24 h was attained, with a matched time kill kinetics against the *P. aeruginosa* bacteria. CS1 loaded films were determined more effective than the CS4-loaded or the unloaded surfaces. Future work will be aimed at improving the loading capacity and homogeneity of the microcapsules, so a more effective antimicrobial profile and prolonged release can be achieved.

Author Contributions: conceptualization, C.S.M., J.C.A., N.C.H.; writing original draft, C.S.M.; revision and editing, J.C.A., N.C.H., H.P.F.; supervision, N.C.H., H.P.F.; funding acquisition, H.P.F. All authors have read and agreed to the published version of the manuscript.

Acknowledgments: Authors acknowledge the Portuguese Foundation for Science and Technology (FCT), FEDER funds by means of Portugal 2020 Competitive Factors Operational Program (POCI) and the Portuguese Government (OE) for funding the project PEPTEX with reference PTDC/CTM-TEX/28074/2017 (POCI-01-0145-FEDER-028074). Authors also acknowledge project UID/CTM/00264/2020 of Centre for Textile Science and Technology (2C2T), funded by national funds through FCT/MCTES. C.S.M. acknowledges FCT for the PhD grant with reference 2020.08547.BD. SEM studies were performed at the Materials Characterization Services of the University of Minho (SEMAT/UM).

Conflicts of Interest: The authors declare no conflict of interest.

References

1. Wu, W.; Jin, Y. et al. Pseudomonas aeruginosa. *Elsevier Ltd.* **2014**, doi:10.1016/B978-0-12-397169-2.00041-X.
2. Buhl, M.; Peter, S.; Willmann, M. Prevalence and risk factors associated with colonization and infection of extensively drug-resistant Pseudomonas aeruginosa: A systematic review. *Expert Rev. Anti. Infect. Ther.* **2015**, *13*, 1159–1170, doi:10.1586/14787210.2015.1064310.
3. Sader, H.S.; Jones, S.R. Antimicrobial susceptibility of uncommonly isolated non-enteric Gram-negative bacilli. *Int. J. Antimicrob. Agents*.**2005**, *25*, 95–109, doi:10.1016/j.ijantimicag.2004.10.002.
4. Felgueiras, H.P.; Homem, N.C.; Teixeira, M.A.; Ribeiro, A.R.; Antunes, J.C.; Amorim, M.T.P. Physical, thermal, and antibacterial effects of active essential oils with potential for biomedical applications loaded onto cellulose acetate/polycaprolactone wet-spun microfibers. *Biomolecules* **2020**, *10*, 1–20, doi:10.3390/biom10081129.
5. MacLean, R.C.; Millan, A.S. The evolution of antibiotic resistance. *Science* **2019**, *365*, 1082–1083, doi:10.1126/science.aax3879.

6. Tavares, T.D.; Antunes, J.C. Biofunctionalization of Natural Fiber-Reinforced Biocomposites for Biomedical Applications. *Biomolecules* **2020**, 10, doi:10.3390/biom10010148.
7. Omonijo, F.A.; Ni, L.; Gong, J.; Wang, Q.; Lahaye, L.; Yang, C. Essential oils as alternatives to antibiotics in swine production. *Anim. Nutr*. **2018**, *4*, 126–136, doi:10.1016/j.aninu.2017.09.001.
8. Miranda, C.S.; Ribeiro, A.R.M.; Homem, N.C.; Felgueiras, H.P. Spun Biotextiles in Tissue Engineering and Biomolecules Delivery Systems. *Antibiotics* **2020**, doi:10.3390/antibiotics9040174.
9. Deng, S.; Gigliobianco, M.R.; Censi, R.; Di Martino, P. Polymeric nanocapsules as nanotechnological alternative for drug delivery system: Current status, challenges and opportunities. *Nanomaterials* **2020**, *10*, 1–39, doi:10.3390/nano10050847.
10. Frank, L.A.; Gazzi, R.P.; de Andrade Mello, P.; Buffon, A.; Pohlmann, A.R.; Guterres, S.S. Imiquimod-loaded nanocapsules improve cytotoxicity in cervical cancer cell line. *Eur. J. Pharm. Biopharm*. **2019**, *136*, 9–17, doi:10.1016/j.ejpb.2019.01.001.
11. Pohlmann, A.R.; Weiss, V.; Mertins, O.; da Silveira, N.P.; Guterres, S.S. Spray-dried indomethacin-loaded polyester nanocapsules and nanospheres: Development, stability evaluation and nanostructure models. *Eur. J. Pharm. Sci*. **2002**, *16*, 305–312, doi:10.1016/S0928-0987(02)00127-6.
12. Chen, H.; Wang, L.; Yeh, J.; Wu, X.; Cao, Z.; Wang, Y.A.; Zhang, M.; Yang, L.; Mao, H. Reducing non-specific binding and uptake of nanoparticles and improving cell targeting with an antifouling PEO-b-PγMPS copolymer coating. *Biomaterials* **2010**, *31*, 5397–5407, doi:10.1016/j.biomaterials.2010.03.036.
13. Jeon, S.J.; Oh, M.; Yeo, W.S.; Galvao, K.N.; Jeong, K.C. Underlying mechanism of antimicrobial activity of chitosan microparticles and implications for the treatment of infectious diseases. *PLoS ONE* **2014**, *9*, doi:10.1371/journal.pone.0092723.
14. Benhabiles, M.S.; Salah, R.; Lounici, H.; Drouiche, N.; Goosen, M.F.A.; Mameri, N. Antibacterial activity of chitin, chitosan and its oligomers prepared from shrimp shell waste. *Food Hydrocoll*. **2012**, *29*, 48–56, doi:10.1016/j.foodhyd.2012.02.013.
15. Sarker, B.; Papageorgiou, D.G.; Silva, R.; Zehnder, T.; Gul-E-Noor, F.; Bertmer, M.; Kaschta, J.; Chrissafis, K.; Detsch, R.; Boccaccini, A.R. Fabrication of alginate-gelatin crosslinked hydrogel microcapsules and evaluation of the microstructure and physico-chemical properties. *J. Mater. Chem*. B. **2014**, *2*, 1470–1482, doi:10.1039/c3tb21509a.
16. Dong, Z.; Wang, Q.; Du, Y. Alginate/gelatin blend films and their properties for drug controlled release. *J. Memb. Sci.* **2006**, *280*, 37–44, doi:10.1016/j.memsci.2006.01.002.
17. Boontheekul, T.; Kong, H.J.; Mooney, D.J. Controlling alginate gel degradation utilizing partial oxidation and bimodal molecular weight distribution. *Biomaterials*. **2005**, *26*, 2455–2465, doi:10.1016/j.biomaterials.2004.06.044.
18. Balakrishnan, B.; Jayakrishnan, A. Self-cross-linking biopolymers as injectable in situ forming biodegradable scaffolds. *Biomaterials* **2005**, *26*, 3941–3951, doi:10.1016/j.biomaterials.2004.10.005.
19. Bigi, A.; Panzavolta, S.; Rubini, K. Relationship between triple-helix content and mechanical properties of gelatin films. *Biomaterials* **2004**, *25*, 5675–5680, doi:10.1016/j.biomaterials.2004.01.033.
20. Boccafoschi, F.; Ramella, M.; Fusaro, L.; Catoira, M.C.; Casella, F. Biological grafts: Surgical use and vascular tissue engineering options for peripheral vascular implants. *Elsevier* **2018**, doi:10.1016/B978-0-12-801238-3.10997-3.
21. Tavares, T.D.; Antunes, J.C.; Padrão, J.; Ribeiro, A.I.; Zille, A.; Amorim, M.T.P.; Ferreira, F.; Felgueiras, H.P. Activity of specialized biomolecules against gram-positive and gram-negative bacteria. *Antibiotics*. **2020**, *9*, 1–16, doi:10.3390/antibiotics9060314.
22. Hill, L.E.; Gomes, C.; Taylor, T.M. Characterization of beta-cyclodextrin inclusion complexes containing essential oils (trans-cinnamaldehyde, eugenol, cinnamon bark, and clove bud extracts) for antimicrobial delivery applications. *LWT Food Sci. Technol*. **2013**, *51*, 86–93, doi:10.1016/j.lwt.2012.11.011.
23. Kirisits, M.J.; Prost, L.; Starkey, M.; Parsek, M.R. Characterization of Colony Morphology Variants Isolated from. *Am. Soc. Microbiol*. **2005**, *71*, 4809–4821, doi:10.1128/AEM.71.8.4809.
24. Nazzaro, F.; Fratianni, F.; De Martino, L.; Coppola, R.; De Feo, V. Effect of essential oils on pathogenic bacteria. *Pharmaceuticals* **2013**, *6*, 1451–1474, doi:10.3390/ph6121451.
25. Lazcano, A. What is life.pdf. **2002**, *46*, 1914–1920, doi:10.1128/AAC.46.6.1914.